

## A Tool for the Simulation of Turbo-Machine Auxiliary Lubrication Plants

L. Pugi<sup>a\*</sup>, R. Conti<sup>a</sup>, D. Nocciolini<sup>a</sup>, E. Galardi<sup>a</sup>, A. Rindi<sup>a</sup> and S. Rossin<sup>b</sup>

<sup>a</sup>Department of Industrial Engineering, University of Florence, Florence, Italy; <sup>b</sup>General Electric Nuovo Pignone srl, Florence, Italy

The reliability and safety of large turbo-machinery systems used in the oil and gas industries are heavily affected by the efficiency of the lubrication plant. In particular, hazard and operability (HAZOP) analyses are often performed using piping and instrumentation diagrams (P&ID; according to regulations in force, ISO 14617). Usually, these analyses are time-consuming and affected by potentially dangerous errors. In this work, a tool for the mono-dimensional simulation of thermal hydraulic plants is presented and applied to the analysis of safety-relevant components of compressor and pumping units, such as the lubrication circuits. Compared to known commercial products, the proposed tool is optimised for fixed step solvers in order to make real-time (RT) integration easier. The proposed tool defines a general approach, and can be used as a SimScape-Simulink library of thermal-hydraulic components (designed according to the P&ID definitions). Another interesting feature of the tool is the automatic scheme generation, where the Simulink model can be automatically generated by P&ID schemes.

**Keywords:** real time code prototyping; lube oil console; rotating machinery; Hazard and Operability analysis; transient behaviour analysis

### 1. Introduction

The objective of this work is the development of an integrated tool, somewhere between CAD software and simulation, for the mono-dimensional analysis and simulation of thermal-hydraulic systems (Karnopp and Rosenberg, 1975; Bouamama, 2003; Kulakowski et al., 2007). Specifically, the tool was developed in a Matlab-Simulink<sup>®</sup> environment, and has been customised for the simulation of lube oil plants during virtual hazard and operability (HAZOP) analysis (Crawley et al., 2008). The tool, called the Virtual HAZOP Toolbox, is the result of the cooperation between the University of Florence (in particular the Mechatronics and Dynamic Modelling Lab) and the industrial partner, General Electric Oil and Gas Nuovo Pignone (Florence, Italy).

Currently, thermal-hydraulic simulations are performed by established commercial software, such as Mentor Graphics Flowmaster<sup>®</sup>, LMS Amesim<sup>®</sup>, or Aspen Hysys<sup>®</sup>, which have been validated by many users in both the academic and industrial fields. This paper represents a feasibility study of an innovative piece of software – the Virtual HAZOP Toolbox – for introducing the concept of failure analysis. Moreover, the software can be seen as a halfway point between the CAD environment and simulation. In particular, as an initial step for introducing the automatic failure analysis, different failures will be analysed and compared with the experimental data to verify the robustness of the system.

The main requirements to integrate virtual HAZOP analysis into the product workflow are:

- *Automatic model generation:* a simulation model can be automatically generated, assembling a pre-defined population of submodels from a technical database and documentation available in the internal P&ID, CAD tool PidXp<sup>™</sup>. The automatic model generation from plant sketches reduces errors introduced by data transcriptions and operator error. However, the consistency of exchanged data by the assembled submodels must be verified by the end user.
- *Hardware in the Loop (HIL) and Software in the Loop (SIL) simulation (Mark VIe Control co-simulation):* the HIL-SIL approach is used for the development and for the verification of controllers such as Mark VIe. Consequently, it is important to maintain the compatibility with Mathworks<sup>®</sup> tools that support automatic code generation for different targets.

Considering the above-mentioned applications, two main requirements of the tool have to be assured:

*Optimisation for Fixed Step solvers and RT implementation:* considering the previously described use for HIL-SIL testing, the tool is used for the fast prototyping of RT code. This application involves the use of fixed-step solvers to obtain a deterministic task time with predefined computational resources. Also, automatic generation of C-code for a RT target is supported.

---

\*Corresponding author. Email: [luca.pugi@unifi.it](mailto:luca.pugi@unifi.it)

*Robustness*: the tool will be used to simulate virtual HAZOP analysis (component failures or off-design conditions) during the design process. These critical situations often correspond to a poor numerical conditioning of the simulation parameters.

## 2. Description of the equations

### 2.1 Fluid properties: Approximated polynomial formulation

One of the aims of the proposed tool is to simulate the thermal hydraulic transient of a plant, considering off-design conditions, which are often associated to pressure–temperature working ranges where the fundamental properties of the fluids such as viscosity and density could change in an appreciable way.

In particular, in the Virtual HAZOP Toolbox, the real behaviour of the fluid is modelled, considering the physical variables as polynomial functions of fluid pressure and temperature, and extrapolating the fluid properties with respect to  $p_{ref}$  and  $T_{ref}$  conditions:

- Specific volume  $v_s$  is interpolated with a second-order polynomial law:

$$V_s = \frac{1}{\rho} = v_{so} \left[ 1 + a_{p1}(p - p_{ref}) + a_{p2}(p - p_{ref})^2 + a_{t1}(T - T_{ref}) + a_{t2}(T - T_{ref})^2 + a_{pt}(p - p_{ref})(T - T_{ref}) \right]; \quad (1)$$

- Absolute viscosity  $\mu$  is approximated by an exponential law whose exponent is interpolated with a second-order polynomial law:

$$\mu = \mu_0 10^\psi; \quad \psi = b_{p1}(p - p_{ref}) + b_{t1}(T - T_{ref}) + b_{t2}(T - T_{ref})^2; \quad (2)$$

- Specific heat coefficient  $c_p$  is interpolated with a second-order polynomial law:

$$c_p = c_{po} \left[ 1 + c_{t1}(T - T_{ref}) + c_{t2}(T - T_{ref})^2 + c_{p1}(p - p_{ref}) + c_{pt}(p - p_{ref})(T - T_{ref}) \right]; \quad (3)$$

- Thermal Conductivity  $\lambda$  sensitivity against pressure is neglected:

$$\lambda_p = \lambda_{po} \left[ 1 + d_{t1}(T - T_{ref}) + d_{t2}(T - T_{ref})^2 \right]. \quad (4)$$

The main advantages of the proposed approach are the simplicity of the equations, obtained using Taylor series in the linearisation process, and the possibility of describing in a closed form the partial derivative of pressure and temperature (which are more suitable from a computational point of view).

### 2.2 Discretisation of the system

The general approach followed in the literature (Merrit, 1967; Karnopp and Rosenberg, 1975; Manring, 2005; Kulakowski et al., 2007), for a mono-dimensional flow, is described in terms of mass conservation, momentum, and enthalpy balances based on Eqs. 5–7:

$$\frac{d\rho}{dt} = \frac{\frac{dm}{dt} - \rho \frac{dV}{dt}}{V(t)}; \quad (5)$$

$$\rho \left( \frac{\partial v_x}{\partial t} + v_x \frac{\partial v_x}{\partial x} \right) = - \frac{\partial p}{\partial x} - f_x; \quad (6)$$

$$\frac{dh}{dt} = c_p \frac{dT}{dt} - T \left( \frac{\partial v_s}{\partial T} \right)_p \frac{dp}{dt}. \quad (7)$$

In order to reproduce the dynamic behaviour of thermal hydraulic systems, partial differential equations (PDEs) – Eqs. 5–7 – are solved. Following the approach, similar to the suggested examples in Karnopp and Rosenberg (1975), Bouamama (2003), and Kulakowski et al. (2007), and usually adopted by commercial software (LMS Amesim Technical Documentation), the plant is discretised in lumped elements where the PDEs (Eqs. 5–7) are rewritten in terms of control volume balances. Therefore, the system can be described by an ordinary differential equation (ODE) system. The main components are:

- *A resistive and inertial (RI) element*: a lumped component where only the momentum balance is implemented, in order to calculate the mass flow rate and the enthalpy flow rate. The control sections, considering inlet and outlet conditions (pressure and temperature), are imposed by an external source or calculated by an adjacent capacitive element. If transient terms (time derivative) in Eq. 6 are neglected, only dissipative effects are modelled and the corresponding element is called *R* or pure resistive element as can be seen in Fig. 1.
- *Capacitive (C) element*: a lumped volume (or capacity) where energy and mass balances are performed to calculate a local value of  $T$  and  $p$  (assuming inlet and outlet mass flow rates  $Q_m$ , and enthalpy flow rates  $Q_h$  as imposed). Moreover, both the thermal and the work exchanges can be considered, introducing in Eqs. 5 and 7 the corresponding effects (as shown in Fig. 1).
- *T and special junction blocks*: since complex hydraulic circuits are composed of networks with

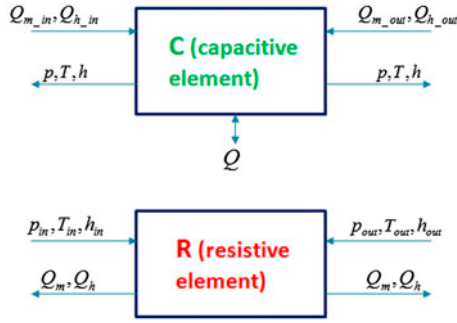


Figure 1. Description of the resistive and capacitive elements.

several loops, hybrid elements (composed of resistive and capacitive elements) are used to connect multiple loops.

- *Imposed source block*: to impose boundary conditions as, for example, an assigned pressure–temperature source or an assigned mass flow rate, simple terminator blocks should be added to the simulation scheme.

### 2.3 Resistive equations

As shown in Fig. 2, considering a uniform flow rate in a pipe with a constant section  $A$ , length  $l$ , inclined to an angle  $\alpha$  with respect to the ground, the momentum balance, shown in Eq. 6, should be written as in Eq. 8, where  $Q_v$  is the volumetric flow rate ( $\text{m}^3/\text{s}$ ) assumed to be homogenous along the pipe:

$$\rho l \frac{dQ_v}{dt} = (p_1 - p_2) A - \xi(Re) \frac{\rho |Q_v| Q_v}{2A} - \rho g \sin(\alpha) Al. \quad (8)$$

The  $\xi$  term represents the viscous friction factor which is calculated as a function of Reynolds number. In the form described by Eq. 8, the volumetric flow rate can be calculated by means of the integration layout schematised in Fig. 2.

However, in several examples, as the contribution of the time derivative terms are negligible, Eq. 8 can be written in a simpler form (shown in Eq. 9) that can be solved without any additional integrator block. In that case, the element is simply called  $R$  (or “pure resistive”) and corresponds to a simpler implementation.

$$(p_1 - p_2) A - \xi(Re) \frac{\rho |Q_v| Q_v}{2A} - \rho g \sin(\alpha) Al = 0; \quad Q_v = f(p_1, p_2). \quad (9)$$

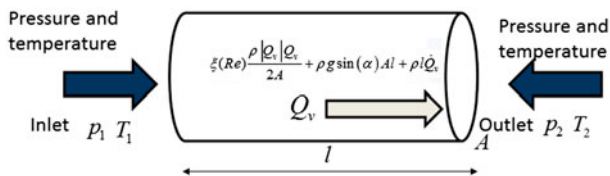


Figure 2. Sketch of a general RI element.

Losses in equation (9) are modelled according the approach proposed by Duqiang. The mass flow rate  $Q_m$  is directly calculated from the volumetric flow rate  $Q_v$  and the density value in the inlet section. In addition, considering the iso-enthalpy hypothesis of the flow, the enthalpy flow rate is computed starting from the specific enthalpy.

$$Q_m = \rho Q_v; \quad (10)$$

$$Q_h = h Q_m; \quad (11)$$

The use of the  $R$  and the  $RI$  components allows the simulation of different components such as distributed or lumped pipe losses, orifices, and valves, which can be defined through a variable area (flow coefficient). The controlled  $R$  components consist of systems which have the controller algorithm implemented using the Matlab–Simulink® blocks.

It is worth noting the possibility of modelling hydraulic actuators (such as pumps and motors) using a customised version of Eq. 9, where  $Q_v$  is directly calculated to model actuator behaviour: i.e. a centrifugal pump is described in terms of load  $\phi$  and flow  $\psi$  coefficients. Hence, Eq. 12 should be adopted:

$$\begin{aligned} Q_v &= f(p_1, p_2, n) = f(\phi, \psi, n); \quad \phi(\psi) = \frac{Q_v}{nc_\phi}; \\ \psi &= \frac{p_1 - p_2}{n^2 c_\psi}; \quad n \\ &= \text{rotation speed}; \quad c_\phi, c_\psi, \text{ characteristic coefficients.} \end{aligned} \quad (12)$$

Enthalpy exchanges introduced by the hydraulic actuators have to be evaluated for the calculation of the proper enthalpy flow rate; indeed, the specific enthalpy  $h$  in the outlet section has to be coherently recomputed taking into account the exchanged mechanical work calculated in Eq. 7. Even considering the hydraulic power  $W_h$  and the efficiency of the pump  $\eta(\phi, \psi)$ , it is possible to compute the mechanical power  $W_m$  and the required torque  $T_m$ . As a consequence, a pump or an actuator/motor should also be modelled as a customised resistive block.

### 2.4 Capacitive equations

The mass conservation in Eq. 5 can be applied to a control volume represented in Fig. 3 to determine the density  $\rho$  and, consequently, knowing the properties of the modelled fluid, it is possible to calculate the pressure derivative from Eq. 13.

$$\begin{aligned} \frac{dp}{dt} &= \beta \left[ \frac{1}{\rho} \frac{d\rho}{dt} + \alpha \frac{dT}{dt} \right] = \beta \left[ -\frac{1}{v_s} \frac{dv_s}{dt} + \alpha \frac{dT}{dt} \right]; \text{ with} \\ &: \begin{cases} \alpha = -\frac{1}{\rho} \left( \frac{\partial \rho}{\partial T} \right)_p = \frac{1}{v_s} \left( \frac{\partial v_s}{\partial T} \right)_p \\ \beta = \frac{\rho}{\left( \frac{\partial p}{\partial p} \right)_T} = \frac{1}{v_s} \left( \frac{\partial p}{\partial p} \right)_T = \frac{-v_s}{\left( \frac{\partial v_s}{\partial p} \right)_T} \end{cases} \end{aligned} \quad (13)$$

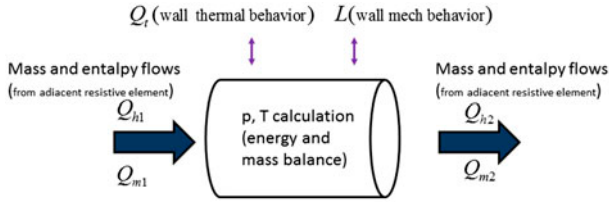


Figure 3. Control volume considered for mass and enthalpy balance.

where  $v_s$  is the specific volume. In Eq. 13, the  $\alpha$  coefficient appears that takes into account the thermal dilatation of the fluid.

Temperature derivative is calculated from enthalpy balance shown in Eq. 7, which is written in simplified form in Eq. 14:

$$\frac{dT}{dt} = \frac{Q_{h1} - Q_{h2} - \rho(dV/dt)h + Q_T + L}{Vc_p} v_s + \frac{1}{c_p} T \left( \frac{\partial v_s}{\partial T} \right)_p \frac{dp}{dt}. \quad (14)$$

Therefore, both pressure and temperature profiles are homogenous in the control volume. They can be calculated by integrating Eqs. 13 and 14 according to the simplified scheme in Fig. 3.

The exchanges between the capacitive element and the external environment are allowed both by the  $Q_t$  (heat exchanged, i.e. the heat flow due to the non-adiabatic capacitive) and by the external work  $L$  (i.e. the mechanical work of an hydraulic actuator). The change of the volume capacity, due to the wall flexibility, is modelled through a wall function  $V(p)$ .  $V(p)$  calculates the internal volume derivative considering the internal pressure coupled with the external mechanical impedance. Therefore, the effect of a generic real pipe wall with an elastic behaviour is modelled, or alternatively (customising the  $V(p)$  function), a simple effect actuator coupled with a mechanical impedance can be modelled.

A variable volume or pressurised tanks is also modelled as particular case of capacitive elements by properly modelling the  $V(p)$  function. It is interesting to note that the heat exchange phenomena are modelled through capacitive blocks.

### 3. Thermal-hydraulic tool implementation

#### 3.1 Simulink–Simscape implementation

High compatibility and interoperability with engineering tools are product specifications. Therefore, the Virtual HAZOP Toolbox is developed as a standard Matlab–Simulink–Simscape<sup>®</sup> library where lumped capacitive or resistive components are modelled as individual blocks. Components that are more complex are implemented as a combination of capacitive and resistive elements.

Code is optimised for RT execution, considering fixed-step computation and compatibility with almost all the supported target compilers.

The blocks inside the Virtual HAZOP Toolbox are masked as standard Simulink components to guarantee that the parameters customisation can be managed with no need for additional knowledge for the standard user. Moreover, the implementation of a physical network involves a bidirectional data exchange between discrete capacitive and resistive lumped elements.

Mathworks<sup>®</sup> has its own tool for the simulation of multi-physic networks (commercially known Simscape<sup>®</sup>), and the bidirectional data exchange between blocks is performed using customised Simscape<sup>®</sup> signals. In this way, complete compatibility is also assured between the Virtual HAZOP Toolbox and the corresponding multi-physics tools of Mathworks<sup>®</sup> (also including solvers optimised for the simulation of physical networks). The command signals or the access to internal states of the component are implemented as standard Simulink input–output port. The graphical aspect of each component is decided by graphical commands that can be changed according to the desired standard used for plant designing such as ANSI Y32.10 (commonly used for fluid power applications) or P&ID (Piping and instrument diagram), mostly derived from ISA standard S5.1 Instrumentation Symbol Specifications.

#### 3.2 Lumped pipe models

Pipes are modelled combining lumped RI, R, and C components, since different kinds of pipe models should be used according to the level of required accuracy. Different pipe sub-models are available, i.e. multiple C-R or C-RI components are usable. As default, pipe connections are generated using a single C component, compatible with the adjacent connected elements.

#### 3.3 Automatic model generation

In order to reduce errors and delays due to model transcription and data transcription from technical documentation, the Simulink model can be automatically generated by P&ID schemes taken from PidXp<sup>™</sup> configuration tool (an engineering tool/database for the definition and sketch of hydraulic systems). Using a simple tool, the user is able to extract automatically a network topology from a P&ID scheme of the hydraulic system, where each component is associated with the corresponding database of properties and technical information, and allows the automatic generation of the model using remote construction instructions. The topology of the automatically generated model is very similar to the P&ID scheme, since there is 1:1 correspondence among P&ID symbols and the dynamical models. PidXp<sup>™</sup> is an AutoCad add-on which introduces several functionalities and produces a drawing file. The automatic conversion tool consists of two parts: the Netlist generator and the XML drawer. The Netlist is a functional net in which all the blocks are connected in terms of their functionalities and connections. The XML drawer is a visual tool able

to visualise the Netlist and modify it. Even relative positions of components are reproduced to define an intuitive approach. Since the model is created in Matlab–Simulink<sup>®</sup>, further customisation and modifications are still possible, considering that most of the parameters are masked and the blocks are accessible as standard masked subsystems. The workflow corresponding to the automatic model generation from PidXp<sup>™</sup> is schematised in Fig. 4.

It is interesting to note that the software is designed with a modular approach so expert users may directly drop blocks to produce their own heavily customised code for simulation.

On the other hand, standard analysis can be also performed by intermediate and entry-level users following an automated-guided process which drastically reduces the risk of human error and assures a safe and repeatable method of working.

### 3.4 Optimising integration and solving methods

The Virtual HAZOP Toolbox is implemented in Matlab–Simulink<sup>®</sup>, and all the supported solvers can be used. However, considering code optimisation and benchmark tests executed by the authors, there are some considerations.

Simulations of thermo-hydraulic systems (and more generally of multi-physics systems) involve a range of problems:

- Numerical stiffness: i.e. associated with the rigid behaviour of the fluid (nearly incompressible).

- Non-linear behaviour: a hydraulic plant is composed by elements with highly non-linear behaviour which often produce strong discontinuities in the solutions.
- Mixed differential algebraic equations (DAE) and ordinary differential equations (ODE): combinations of both DAE and ODE equations involve the use of a very robust solver.

Since the feasibility of RT simulation represents an important specification, the authors have optimised the code in order to privilege robustness when fixed-step solvers are used and limited computational resources are available, involving the use of low sampling-solving frequencies.

For this kind of application, implicit solvers were more stable than explicit ones; in particular, the ‘ode14x’ (Matlab–Simulink Technical Documentation), which is an extrapolation solver based on linearly implicit Euler method (Deuffhard et al., 1987; Lubich, 1989) is preferred because it represents the best compromise in terms of stability and numerical efficiency.

Also, a stabilising run (a sort of pre-simulation) should be performed in order to increase the consistency of the imposed initial conditions and consequently to avoid potential numerical problems in the model initialisation phase.

Efficiency and stability problems also arise in virtual HAZOP analysis where long or multiple simulation patterns need to be performed in which different or worst-case scenarios have to be analysed. Even in this case, stability is a difficult issue, since the simulation of

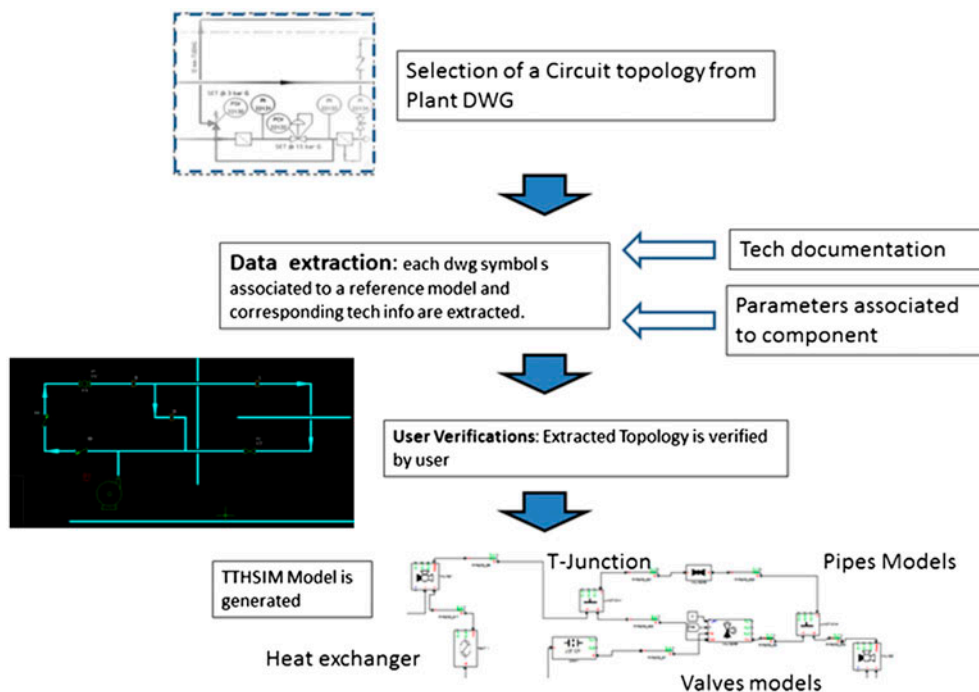


Figure 4. Typical workflow from P&ID scheme to the corresponding Virtual HAZOP Toolbox.

“stressed” plants often involves the implementation of poorly conditioned physical systems operating in a failure situation which is far from the nominal one.

In this case, it is possible to change the integrator parameters (time integration step, tolerance, etc.) in the simulation instant, near to the transition between the steady state in nominal conditions and the failure situation. Hence, a long time integration step (low integration frequency) can be applied to the simulation in nominal plant conditions, saving the simulink integrators’ state in a stable and coherent configuration. Then, starting from the previously saved simulink state and the correctly initialised integrators, a short time integration step (high integration frequency) can be associated with the simulation in critical conditions (failures).

#### 4. Virtual HAZOP: Preliminary validation

The debugging and the validation phases are quite onerous tasks which can be preliminary performed by means of several benchmark cases, analysed with the GE supervisors, obtaining direct feedback in terms of knowledge, practice, and experimental data from the existing plants.

An initial debug of the code is performed, comparing the results obtained by the Virtual HAZOP Toolbox and a commercial code on a simplified benchmark model. Preliminary cross-verification with a commercial code is considered mandatory in order to verify the numerical performance and correctness of the implementation on known assigned models. Since some components may not be differently implemented on the commercial code, coherence between the two models is carefully verified.

In the virtual HAZOP procedure, the main physical variables evaluated from the user are:

- *Load pressure*: the load pressure is measured at the output of the lube oil console.
- *Collector pressure*: the pressure measured at the intersection between the two pumps.
- *Main pump pressure*: the pressure measured at the outlet of the main pump.
- *Auxiliary pump pressure*: the pressure measured at the outlet of the auxiliary pump.
- *TCV temperature*: the temperature after the temperature control valve (TCV).

In this work, authors focused on the plant described in Fig. 5

The hydraulic load, i.e. the bearing of a turbo-machine, is modelled as an equivalent orifice (load in Fig. 5), which is fed with an assigned inlet pressure. The inlet pressure is self-regulated by a pressure control valve (PCV). The inlet flow to the PCV is assured by a centrifugal pump moved by an asynchronous motor. In case of failure, to increase the system reliability, a parallel auxiliary pump is available.

Asynchronous motor is modelled considering a known-tabulated speed–torque response  $T_e(n)$  provided by GE NP and a filtering transfer function is introduced to model inertial and viscous friction mechanical loads, as shown in Eq. 15:

$$T_e(n) - T_m = J_m \frac{dn}{dt} + f_n \implies n = \frac{T_e(n) - T_m}{J_m s + f}; J_m = \text{mech. inertia}; f = \text{friction factor.} \quad (15)$$

During the failure of the pump, the pressure of the PCV is stabilised by the pressurised tank (GT in Fig. 5).

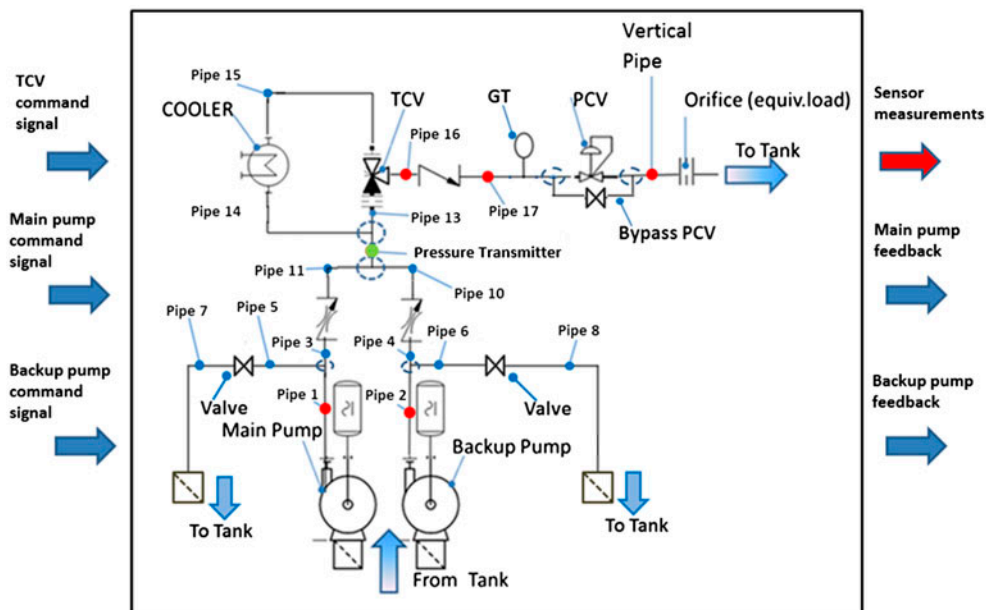


Figure 5. Lube oil console scheme.

A three-way TCV is used to stabilise oil temperature to an assigned value of 50°C by regulating the volumetric flow rate passing through a cooler (modelled as a composite R-C-R component). The cooler is simulated supposing a constant heat exchange coefficient.

The inputs of the lube oil console are the TCV command signal, the main pump, and the auxiliary pump command signal. The outputs are the sensors measurements (highlighted with a red point in Fig. 5 and described above), the main and auxiliary pumps feedbacks.

These signals are passed to the Mark VIe Control model, where by evaluating both the pressures before the equivalent load and in the collector, and the temperature after the TCV, computes the command signals to lube oil console components.

Additional orifices, check valves, and bypass valves are added to the plant in order to simulate other known lumped losses. Pipes are modelled as R-C-R elements (two resistive and a capacitive elements) neglecting the contribution of inertial forces in equations. Main Features of the modelled components are described in Table 1.

Using the simplified model described above, different failures or operating conditions can be simulated. Each component simulates its failure behaviour; i.e. the TCV

can fail both opening the cold inlet only or the hot inlet only, the pump motor can fail because the motor torque is not passed to the centrifugal pump, etc.

In the Virtual HAZOP Toolbox, the failure list is automatically created defining the plant topology and the components. In this preliminary validation, the lube oil console is modelled into the Virtual HAZOP Toolbox and, in the commercial code, by defining the maximum case of the possible failures; the possible scenarios can be increased, since the pressurised gas tanks could be utilised. In Table 2, the failure list is summarised.

All these tests are performed comparing the main physical variables described above. Among the various failures, in this work the authors are focused on the “Pump switch without pressurised tank” failure in order to verify both the controller behaviour and the thermal-hydraulic stability. The experimental data are provided by GE NP.

In Fig. 6, the pressure simulated in the collector point is shown. The collector pressure is acquired by the pressure transmitter. The pump switch is enabled at 15 s, and the controller starts the auxiliary pump when this pressure is under the 7 BarG. In Fig. 7, the load pressure is analysed.

Table 1. Component Parameters.

Component	Parameters	Init. conditions $Q_v(0)[\text{m}^3/\text{s}] - T(0)[\text{C}^\circ]$
Check valve	nominal flow (0.011 m <sup>3</sup> /s) nominal drop (1 bar)	0–43
Check valve with orifice	nominal flow (0.011 m <sup>3</sup> /s) nominal drop (1 bar) orifice diameter (3 mm)	0–43
PCV	orifice diameter (55 mm) pressure setpoint (2.5 barG)	0–43
Pressurised tank	volume (0.6 m <sup>3</sup> ) pre-charge (2.72 barG)	0–43
TCV	orifice diameter (35 mm) temperature setpoint (58°C)	0–43
Cooler	orifice diameter (35 mm) thermal exchange coefficient (7850 WK <sup>-1</sup> )	0–43
Pipe elements	length (3 m) diameter (150 mm)	0–43
Vertical element	length (7 m), diameter (150 mm)	0–43
Centrifugal pump	flow-pressure curve flow-power curve	0–43

Table 2. List of Failures.

Failure	Description
Pump switch without pressurised tank	The main pump is manually switched off to verify the response of the controller. The controller has to activate the backup pump.
Pump switch with pressurised tank	The main pump is manually switched off to verify the response of the controller. The controller has to activate the backup pump.
Opening pump bypass valve without pressurised tank	The pump bypass valve is manually opened to verify the response of the controller. The controller has to activate the backup pump.
Opening pump bypass valve with pressurised tank	The pump bypass valve is manually opened to verify the response of the controller. The controller has to activate the backup pump.
Opening pump bypass valve without pressurised tank with both pumps activated	The pump bypass valve is manually opened to verify the response of the controller.
Opening PCV bypass valve without pressurised tank	The PCV bypass valve is manually opened to verify the response of the controller. The PCV has to become fully open to try to regulate the pressure.
Opening PCV bypass valve with pressurised tank	The PCV bypass valve is manually opened to verify the response of the controller. The PCV has to become fully open to try to regulate the pressure.
Failure cold of the TCV without pressurised tank	The TCV is manually forced to open the cold inlet only.
Failure cold of the TCV with pressurised tank	The TCV is manually forced to open the cold inlet only.

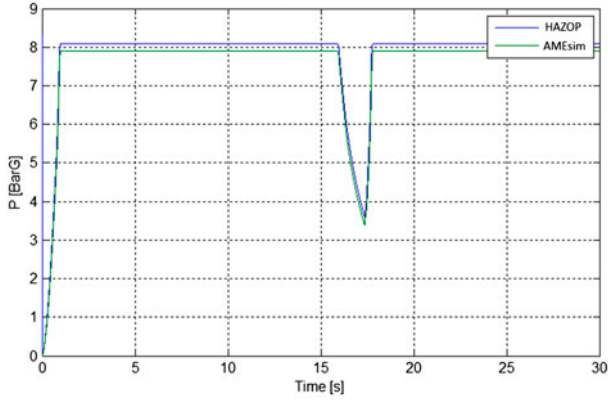


Figure 6. Comparison of the collector pressure between the Virtual HAZOP toolbox and the Amesim model.

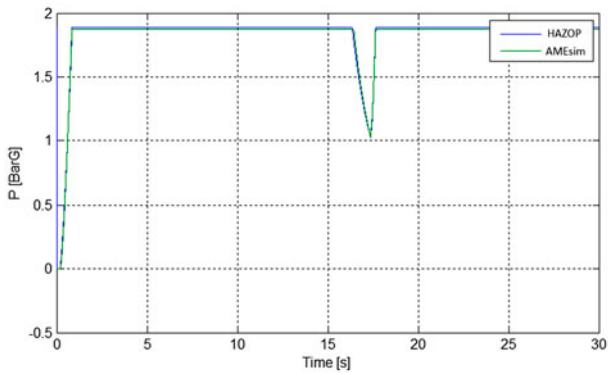


Figure 7. Comparison of the load pressure between the Virtual HAZOP toolbox and the Amesim model.

Finally, in Fig. 8, the comparison between the temperatures measured downstream the TCV is shown. The small differences can be associated with different control or implementation strategies in the two models. The tests performed to evaluate the physical thermal-hydraulic behaviour can be analysed through several indexes:

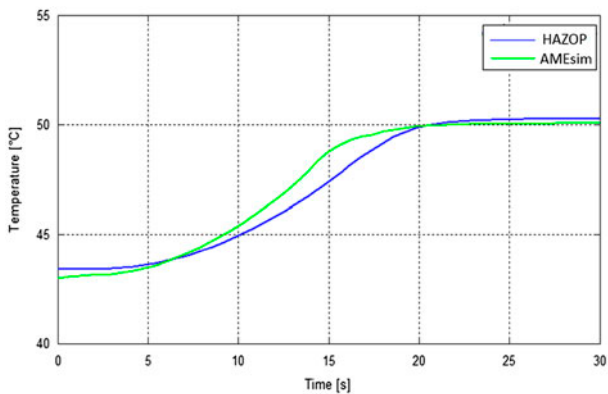


Figure 8. Temperature in the outlet section of the TCV.

- *Load pressure error* ( $E_{LP}$ ): the maximum relative difference between the load pressures calculated by the two pieces of simulation software;
- *Collector pressure error* ( $E_{CP}$ ): the maximum relative error between the collector pressures; and
- *TCV temperature error* ( $E_{TCVT}$ ): the maximum relative error between the two simulated temperatures downstream the TCV.

These indices are used to describe in a synthetic manner the coherency among different tests. In Table 3,  $E_{LB}$ ,  $E_{CB}$  and  $E_{TCVT}$  values, calculated for different failure conditions, show good agreement between the two pieces of simulation software, corresponding to maximum errors of about 2–3%.

The failures in Table 3 represent the main critical situations in which the lube oil console has to be studied; this study represents a significant test case, and can be seen as a feasibility study to understand the failure analyses.

Moreover, to establish the preliminary estimation of efficiency of the implemented code, the running times of both codes are compared considering fixed and variable step implementation as visible in Table 4. Considering variable step implementation, various Matlab–Simulink® “stiff-robust” solvers have been tested, in particular the ‘ode23-tb’ (Matlab–Simulink Technical Documentation). In this case, the solver adopted by the commercial software is two or three times faster than the Virtual HAZOP Toolbox, since the simulation performances are heavily affected by the simulated scenario.

Considering a fixed step implementation (which may be mandatory for RT or HIL applications), the proposed tool exhibits a high stability compared to the chosen integration step which is about  $10^{-4}$  s and can be reduced to  $10^{-3}$  s or less. The same plant, when it is executed using the fixed step solvers of the commercial code, involves the use of a fixed integration step which is typically more than 10 times smaller than the Virtual HAZOP Toolbox.

The corresponding difference in terms of global duration of the simulation is much lower (about 40%); this result is only partially justified by the different kind of solver adopted. Further efforts have to be performed to increase the efficiency of the code and to perform a smarter implementation because the proposed code is still much slower in terms of turnaround time (i.e. the time required to solve a single integration step).

Calculation of computational times is performed considering a standard Notebook with Intel® i7core processor and 8Gb of Ram with a Microsoft Windows7 operating system.

For the Matlab–Simulink® implementation, the use of an *rsim* target (a generic non-RT target which is used to produce a standalone executable of the code) is considered.



Table 3. Error Evaluations.

Failure	$E_{CP}$	$E_{LP}$	$E_{TCVT}$
Pump switch without pressurised tank	2.6%	1.2%	1.8%
Pump switch with pressurised tank	1.3%	1.1%	2.2%
Opening pump bypass valve without pressurised tank	0.7%	0.6%	1.9%
Opening pump bypass valve with pressurised tank	0.9%	0.6%	1.9%
Opening pump bypass valve without pressurised tank with both pumps activated	0.8%	0.6%	1.9%
Opening PCV bypass valve without pressurised tank	1.1%	0.9%	1.8%
Opening PCV bypass valve with pressurised tank	1.0%	0.8%	1.9%
Failure cold of the TCV without pressurised tank	0.9%		1.0%
Failure cold of the TCV with pressurised tank	0.9%		0.9%

Table 4. Comparison of Simulation Performances.

Software	Solver (order)	Solver step (s)	Execution time (s)
Virtual HAZOP toolbox	'ode14x'	$10^{-4}$	174
Commercial	Euler (1)	$10^{-5}$ – $10^{-6}$	290 (minimum)
Commercial	Adams-Bashforth (2)	$2 \cdot 10^{-5}$ – $10^{-6}$	285 (minimum)
Commercial	Runge-Kutta (2)	$2 \cdot 10^{-5}$ – $10^{-6}$	275 (minimum)

## 5. Experimental data

The test case is proposed by GE Nuovo Pignone, and it is referred to a mineral lube oil console usually used to guarantee the proper pressure and mass flow rate to the auxiliary systems of a compressor (in this case, the hydrodynamic journal bearings). In Fig. 9, the test plant (including the lube oil circuit with the two centrifugal pumps and the turbomachine) is shown. In the proposed work, the authors according to GE NP plant designers simulate the bearings as an equivalent orifice.

The objective of this benchmark case is to evaluate both the dynamical behaviour of the thermal-hydraulic system and the Mark VIe Control performance during the pump switch without the pressurised tank. These results will be useful to validate the behaviour simulated through the Virtual HAZOP Toolbox.

Therefore, the aim of the test is to verify the capability of the tool to simulate both a typical transient flow–pressure and a transient temperature in which a relatively fast dynamic behaviour has to be reproduced.



Figure 9. Lube oil plant (courtesy of GE Nuovo Pignone).

The simulation model is obtained through the Virtual HAZOP Toolbox, using the automatic generation of the dynamic model starting from the P&ID scheme.

The test analysed has been carried out during the String Test performed by GE NP in the Massa site. The main parameters to analyse are the load pressure, the collector pressure, the main pump pressure, and the auxiliary pump pressure (pressure transient analysis). Moreover, since the simulation model carries out a thermal-hydraulic analysis, a comparison between the simulated and experimental temperature measured downstream the TCV is evaluated (transient temperature analysis).

The lube oil console model is connected with the Mark VIe Control model (performing a SIL analysis) where all the alarm logics and the controller actions are implemented. The scheme corresponding to the structure of the proposed simulator is shown in Fig. 10.

A first-order low pass filter is applied to every simulated signal, as shown in Eq. 16, which reproduces the dynamic behaviour of the pressure-temperature sensors used on the plant.

$$y(s) = \frac{1}{1 + \tau s} \text{ where } \tau \approx 0.4s(\text{diff. signals}). \quad (16)$$

Simulated failure modes are introduced in the model as programmable input sequences which can be directly controlled by the user or automatically generated by a

failure sequence builder, also implemented in Matlab<sup>®</sup> in order to automate the process.

The validation is carried out by comparing measured pressure profiles, with the corresponding ones calculated using the Virtual HAZOP Toolbox.

In Fig. 11, the behaviour of the main four pressures simulated through the Virtual HAZOP Toolbox is shown. Referring to the lube oil console scheme (in Fig. 10), the comparison between the Virtual HAZOP Toolbox and the experimental data of the collector pressure is shown in Fig. 12.

In Fig. 13, the dynamical behaviour of the main pump after the failure is represented.

The validation process analyses even the transient temperature measured by the temperature sensor downstream the TCV. The transient temperature is greater than the transient pressure due to the thermal inertia of the oil. The TCV is a three-way valve regulated by the Mark VIe Control with a hot and a cold inlet. The data are related to a String Test and provide two different starting points: the first starts at room temperature (about 25°C), while the second starts at a temperature of about 49°C due to the use of preheaters.

The TCV set temperature for both tests is 55°C.

As shown in Fig. 14, the dynamic behaviour of the transient temperature is characterised by rapid heating caused by the preheater in the lube oil tank, then the TCV modulates between the hot and cold entries to obtain the set temperature (55°C).

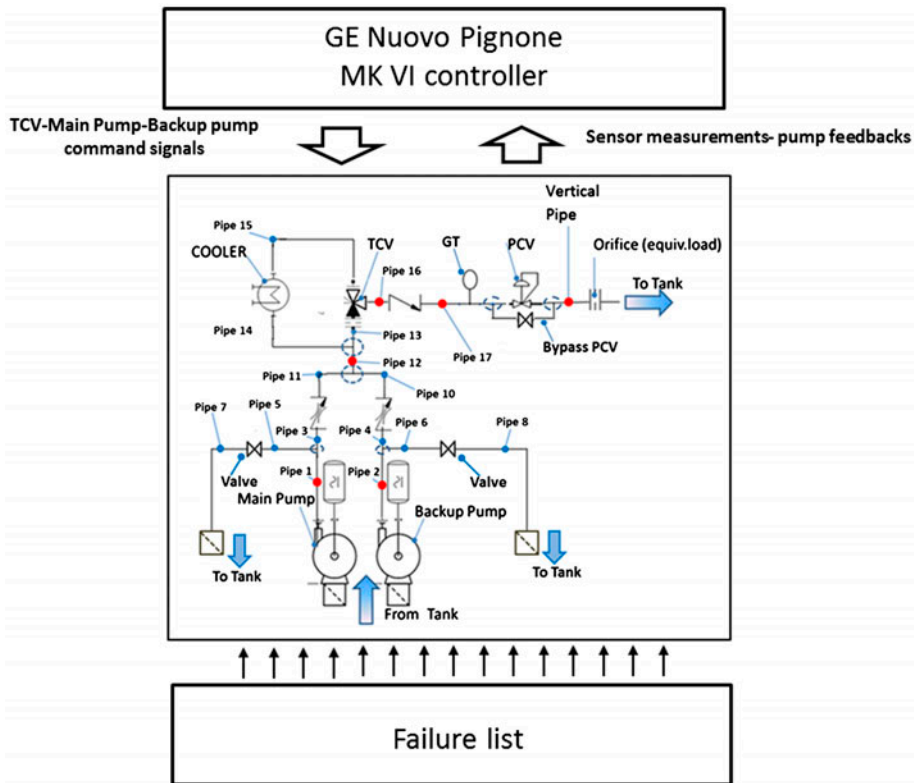


Figure 10. Interactions between the Lube oil console, the model of Mark VIe Control and the failure blocks.

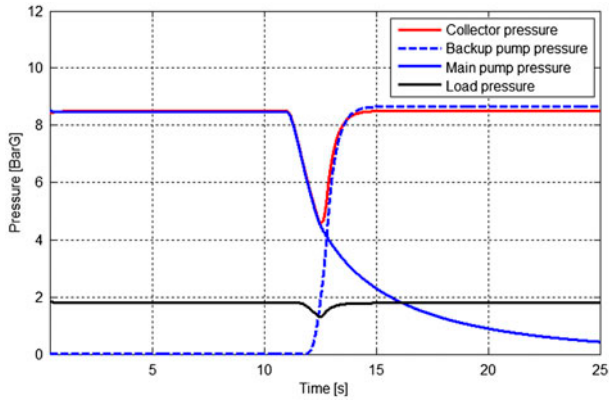


Figure 11. Dynamical behaviour of the main four pressures.

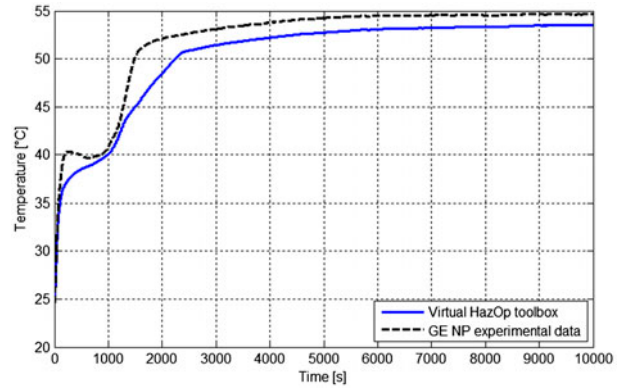


Figure 14. Comparison between the experimental and the simulated data starting from 25°C.

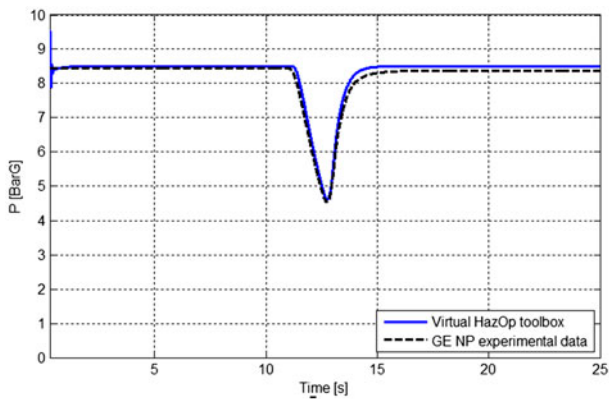


Figure 12. Collector pressures.

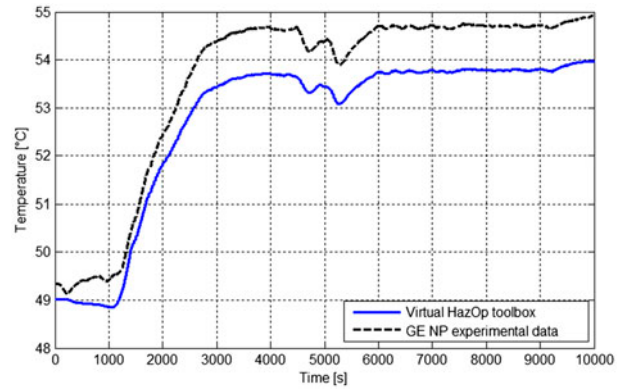


Figure 15. comparison between the experimental and the simulated data starting from 49°C.

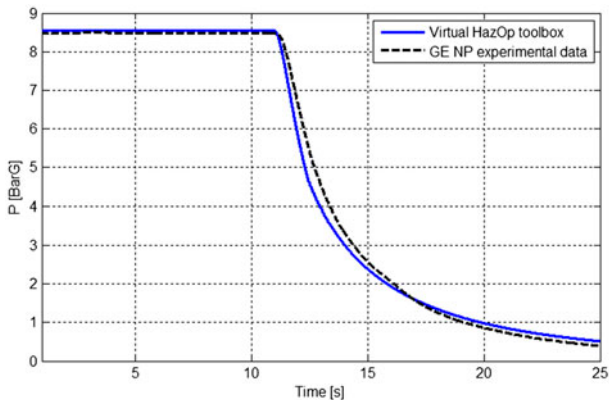


Figure 13. Main pump pressures.

Small differences in the steady state temperature should be justified by an offset and/or by the hysteresis of the valve and the offset of the sensor.

In Fig. 15, starting with a preheated plant, it is possible to see the transient temperature due to the TCV modulation; indeed, in this graph, the offset and the hysteretic behaviour of the valve is clearly shown. In Table 5, the maximum errors among the experimental data and the numerical simulation are summarised.

Table 5. Maximum Errors.

Transmitter	Maximum errors
Collector pressure	<5%
Auxiliary pump pressure	<4%
Main pump pressure	<5%
Load pressure	<4%

### 6. Conclusions and further developments

In conclusion, the authors have implemented a thermal hydraulic toolbox (the Virtual HAZOP Toolbox) in Matlab–Simulink® in which the failure analysis can be completely automatised and which can also be evaluated during the plant design. This work represents a feasibility study to introduce, in the future release of the software, prognostics and health management techniques into the GE NP internal procedures. The PHM techniques allow the study of the failure mechanisms related to system lifecycle management and will be used to drastically reduce the lube oil console economic impacts. Furthermore, inside the Virtual HAZOP Toolbox, the following characteristics are required:

- Optimisation for fixed step solvers and RT implementation;
- Numerical robustness;
- Automatic procedure to convert PIDXp schemes into a Simulink dynamic model; and
- Compatibility with the Mark VIe Control.

The thermal-hydraulic behaviour of the toolbox has been validated by comparing the simulation results with the corresponding ones calculated by commercial software (LMS Amesim<sup>®</sup>). Comparisons have been performed considering several plants and failure scenarios. In parallel with this activity, University of Florence and GE researchers have cooperated to implement the real characteristics of the main components of the lube oil console, e.g. the TCV, the orifices, the PCV, the centrifugal pumps, etc. Finally, the proposed benchmark test case is referred to a mineral lube oil console directly controlled by the Mark VIe Control model that is used to guarantee the desired pressure and flow rate to the auxiliary systems of a compressor plant.

The data acquired by GE NP on a real String Test (test of the whole rotating machinery) showed both the transient pressure during a pump switch and the transient temperature during the start-up of the plant. As a consequence, it has been possible to compare results of a simulated virtual HAZOP with a real application.

The validation process should be completed with a larger population of test results, and probably the number of different components modelled by the Virtual HAZOP toolbox should be further increased. Also the implementation of the models should be further refined in order to increase the robustness and numerical efficiency of the toolbox. In particular, for extended and efficient use of the code, the integration step should be increased to an advisable target of  $10^{-3}/10^{-2}$  seconds. With regard to future developments, an experimental campaign on different lube oil consoles is planned in which the characterisation of the thermal-hydraulic behaviour of the hydrodynamic journal and thrust bearings will be the main focus. In particular, in the actual implementation, bearings are modelled as equivalent orifices with an assigned flow rate–pressure relationship which refers to steady-state nominal working conditions. This is a clear limit for a tool whose main aim is the simulation of off-design conditions and transients which may be much greater than nominal ones.

Currently, the authors are dealing with bibliographic research, and developing the corresponding simulation tools. Further research activities will also be addressed to extend the tool to the simulation of different physical domains such as thermal pneumatics and electro-mechanics systems. In particular, for the modelling of pneumatic systems, the authors' intention is to exploit the previous experience developed with the simulation of railway pneumatic brakes, both with commercial (Pugi, Rindi,

et al., 2011) and customised simulation codes (Pugi, Malvezzi, et al., 2004).

### Acknowledgements

The authors wish to thank all the people of General Electric Nuovo Pignone s.p.a. who helped with this project for their helpful cooperation and competence, and in particular Carmelo Accillaro, Eugenio Quartieri, and Giovanni Lo Presti. The authors also wish to remember the contribution of the student, Alberto Biagini.

### Nomenclature

$A$	Section $m^2$
$c_p$	Specific heat coefficient $J/(kg \cdot K)$
$D$	Diameter mm
$f$	Friction factor –
$f_x$	Axial tangential effort $kg/(m^2 s^2)$
$g$	Acceleration of gravity $m/s^2$
$h$	Specific enthalpy $J/m^3$
$J_m$	Mechanical inertia $kg m^2$
$L$	External work J
$l$	Length m
$m$	Mass kg
$n$	Rotation speed rpm
$p$	Pressure Pa
$Qt$	Heat exchanged J
$Q_h$	Enthalpy flow rate J/s
$Q_m$	Mass flow rate kg/s
$Q_v$	Volumetric flow rate $m^3/s$
$Re$	Reynolds number –
$AT$	Temperature K
$T_e(n)$	Speed-torque response N m
$T_m$	Required torque N m
$V$	Volume $m^3$

$W_h$	Hydraulic power W
$W_m$	Mechanic power W
$\alpha$	Thermal expansion coefficient 1/K
$\beta$	Bulk modulus Pa
$\eta$	Efficiency —
$\lambda$	Thermal conductivity W/(m K)
$\mu$	Absolute viscosity Pa s
$v_s$	Specific volume m <sup>3</sup> /kg
$\zeta(Re)$	Viscous friction factor —
$\phi$	Load coefficient —
$\rho$	Density kg/m <sup>3</sup>
$\tau$	Time constant s
$\psi$	Flow coefficient —

### Notes on contributors



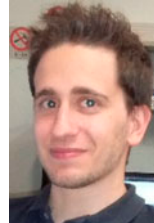
**Luca Pugi** received the degree in mechanical engineering in 1999 from the University of Florence, Florence, Italy, and the Doctorate degree in applied mechanics in 2003 from the University of Bologna, Bologna, Italy. He currently works at the department of industrial engineering, University of Florence, Florence, Italy, where he is involved in design and simulation of mechatronic systems, mainly for vehicle applications collaborating with relevant industrial partners such as General Electric, Trenitalia SPA, Ansaldo Breda, Ansaldo Signal, Pramac SPA, ECM SPA, Velan ABV, Italcertifer SPA, etc. He also performs didactical activities concerning mechatronics and modelling of dynamical systems and electric traction systems. He is the author or co-author of about 170 publications. He is the winner of several international awards: In 2000, the “Cesare Bianchi” award from the Italian Association of Railway Engineers (CIFI), Rome, Italy. In 2009 He was awarded by CIFI with the Mallegori Award. In 2011 at WCRR (World Congress of Railway Research), he was awarded with a premium for the section “increasing freight capacities and services”.



**Roberto Conti** is a Ph.D. Researcher and Assistant Professor of Robotics with the School of Engineering, University of Florence, Florence, Italy. His current research interests include robotics, wearable robotics, and underwater robotics.



**Daniele Nocciolini** is a Ph. D Researcher at the Dept. of Industrial Engineering, University of Florence. His current research interests include Vehicle Dynamics and Mechatronics, including Mechanic and Fluidic Systems.



**Emanuele Galardi** has his Master Degree in Electrical and Automation Engineering and is a Ph.D. researcher at the Dept. of Industrial Engineering, University of Florence. His current research interests are: Control, Vehicle Dynamics and Mechatronics (including Electric, Fluidic and Mechanic Systems).



**Andrea Rindi** was Born in Florence in 1967. In 1996 he has gained his degree in mechanical engineering at University of Florence discussing a thesis concerning an high speed pantograph.

Currently Andrea Rindi works at University of Florence as researcher where he performs didactical activities for the courses of applied mechanics and vehicle dynamics. Currently he coordinates several research projects concerning vehicle dynamics and rotordynamics.



**Stefano Rossin** graduated in 1999 with a M.S. Degree in Aeronautical Engineering at the University Pisa. He began his career early in year 1989 before achieving his M.S. degree in several fields starting from a meteorological research center, moving to a chemical research laboratory and eventually in an Aerospace Company. In 1999, Stefano moved to The Netherlands working for about 6 years as application engineer for a consulting firm on development of complex non-linear computational analysis on structural and fluid flow fields for R&D core businesses of Shell Exploration & Research, Goodyear Tires, Philips, Fokker Aerospace and Xerox.

In August 2005, Stefano joined GE Oil&Gas in Florence (Italy) as Design engineer for the Gas Turbine auxiliary system team and in 2007 promoted to the advanced mechanical analysis leader role. In 2010 Stefano moved to Principal Engineer on Mechanical, piping and Fluid Systems for the Auxiliary system engineering team focusing mainly on Root Cause Analysis and field investigation, and since February 2012 he is holding the position as Consulting Engineering for the GE Oil&Gas Turbo Machinery System engineering organization acting as Subsection Chief engineer for Centrifugal compressors, Gas Turbine and industrial Plant mechanical systems.

He is author of two patents and 10 international papers 2 of which developed in cooperation with important Oil&Gas customers such as Shell Exploration and Exxon Mobil. In June 2013 Stefano received the GE Edison Pioneer Award, an honor presented to one individual selected every year from across GE globally and recognizing mid-career technologists who demonstrate technical excellence and customer impact.

**References**

- Bouamama, B. O. 2003. Bondgraph Approach as Analysis Tool in Thermofluid Model Library Conception. *Journal of the Franklin Institute*, Vol. 340, No. 1, pp. 1–23.
- Crawley, F., Preston, M. and Tyler, B. 2008. *HAZOP Guide to Best Practice*. IChemE, Rugby, UK.
- Deuffhard, P., Hairer, E. and Zugck, J. 1987. One-Step and Extrapolation Methods for Differential-Algebraic Systems. *Numerische Mathematik* Vol. 51, pp. 501–516.
- Duqiang, W., Burton, R., and Schoenau, G. 2002. An Empirical Discharge Coefficient Model for Orifice Flow. *International Journal of Fluid Power*, Vol. 3, No. 3, pp. 13–19.
- Karnopp, D. C. and Rosenberg, R. C. 1975. *System Dynamics*. John Wiley, New York: A Unified Approach.
- Kulakowski, B. T., Gardner, J. F. and Shearer, J. L., 2007. *Dynamic Modelling and Control of Engineering Systems*. 3rd edn. Cambridge University Press, New York, USA.
- LMS Amesim Technical Documentation (online help version 4.1 or later).
- Lubich, C. 1989. Linearly Implicit Extrapolation Methods for Differential-Algebraic Systems. *Numerische Mathematik*, Vol. 55, pp. 197–211.
- Manring, N. D. 2005. *Hydraulic Control Systems*. New York: John Wiley.
- Matlab–Simulink Technical Documentation (online help version 2008A or later).
- Merrit, H. E. 1967. *Hydraulic Control Systems*. New York: John Wiley.
- Pugi, L., Malvezzi, M., Allotta, B., Banchi, L. and Presciani, P. 2004. A Parametric Library for the Simulation of a Union Internationale des Chemins de Fer (UIC) Pneumatic Braking System. *Proceedings of the Institution of Mechanical Engineers, Part F: Journal of Rail and Rapid Transit*, Vol. 218, No. 2, pp. 117–132.
- Pugi, L., Rindi, A., Ercole, A. G., Palazzolo, A., Auciello, J., Fioravanti, D. and Ignesti, M. 2011. Preliminary studies concerning the application of different braking arrangements on Italian freight trains. *Vehicle System Dynamics*, Vol. 49, No. 8, pp. 1339–1365.